# Uremic toxin p-cresyl sulfate enhances the calcification of aortic valvular interstitial cells via klotho/sirtuin-1 signaling

SHAO-JUNG LI[1-5], TZU-YU CHENG[2-4,6], YU-HSUN KAO[3,4,7,8], WEI-YU CHEN[9,10], CHENG-CHIH CHUNG[3-5,11], NGUYEN NGOC TRANG[12], PAO-HUAN CHEN[13,14] and YI-JEN CHEN[3,4,7,11]

[1]Division of Cardiovascular Surgery, Department of Surgery, School of Medicine, College of Medicine, Taipei Medical University, Taipei 110301, Taiwan, R.O.C.; [2]Division of Cardiovascular Surgery, Department of Surgery, Wan Fang Hospital, Taipei Medical University, Taipei 116079, Taiwan, R.O.C.; [3]Cardiovascular Research Center, Wan Fang Hospital, Taipei Medical University, Taipei 116079, Taiwan, R.O.C.; [4]Taipei Heart Institute, Taipei Medical University, Taipei 110301, Taiwan, R.O.C.; [5]Division of Cardiovascular Surgery, Department of Surgery, Shuang Ho Hospital, Taipei Medical University, New Taipei 235041, Taiwan, R.O.C.; [6]Division of Cardiology, Department of Internal Medicine, School of Medicine, College of Medicine, Taipei Medical University, Taipei 110301, Taiwan, R.O.C.; [7]Graduate Institute of Clinical Medicine, College of Medicine, Taipei Medical University, Taipei 110301, Taiwan, R.O.C.; [8]Department of Medical Education and Research, Wan Fang Hospital, Taipei Medical University, Taipei 116079, Taiwan, R.O.C.; [9]Department of Pathology, Wan Fang Hospital, Taipei Medical University, Taipei 116079, Taiwan, R.O.C.; [10]Department of Pathology, School of Medicine, College of Medicine, Taipei Medical University, Taipei 110301, Taiwan, R.O.C.; [11]Division of Cardiovascular Medicine, Department of Internal Medicine, Wan Fang Hospital, Taipei Medical University, Taipei 116079, Taiwan, R.O.C.; [12]Radiology Center, Bach Mai Hospital, Hanoi 100000, Vietnam; [13]Department of Psychiatry, Taipei Medical University Hospital, Taipei 110301, Taiwan, R.O.C.; [14]Department of Psychiatry, School of Medicine, College of Medicine, Taipei Medical University, Taipei 110301, Taiwan, R.O.C.

Received September 15, 2025; Accepted March 3, 2026

DOI: 10.3892/mmr.2026.13872

**Abstract.** Calcific aortic valve disease (CAVD), a valvular heart disease with severe complications, is common in patients with chronic kidney disease (CKD). P-cresyl sulfate (PCS) is a protein-binding uremic toxin that induces chronic inflammation. Klotho and sirtuin-1 (SIRT1) represent potential therapeutic agents for mitigating CKD-induced vascular calcifications. We hypothesized that PCS could enhance valvular interstitial cell (VIC) calcification, which could be modulated by klotho/SIRT1 signaling. Alizarin Red S staining, western blotting and immunohistochemical analysis were performed in order to examine calcification and klotho/SIRT1 signaling in isolated porcine VICs following various 7-day treatments. VIC treatments included incubation with PCS (10 and 100 $\mu$M), klotho (100 pM), the hypoxia-inducible factor-1α (HIF-1α) inhibitor PX-478 (0.5 $\mu$M) and the SIRT1 activator SRT1720 (1 mM). Furthermore, the present study established a PCS-induced rat model of CKD and analyzed the effects of klotho on runt-related transcription factor 2 (RUNX2) expression in rat aortic valves *in vivo*. Treatment with PCS increased VIC calcification, NF-κB acetylation and the expression of RUNX2 and HIF-1α expression but was shown to reduce klotho expression. Klotho supplementation attenuated the PCS-induced enhancement of VIC calcification and mitigated PCS-mediated increases in NF-κB acetylation and RUNX2 expression. Additionally, the SIRT1 activator SRT1720 attenuated the PCS-mediated enhancement of VIC calcification and was shown to upregulate klotho and downregulate RUNX2 in PCS-treated VICs. Furthermore, the present study demonstrated that klotho supplementation mitigated CKD-mediated RUNX2 upregulation in the aortic valves of PCS-treated CKD model rats. The present study demonstrated that PCS induced VIC calcification by activating HIF-1α signaling and downregulating klotho. Treatment with klotho or SRT1720 was shown to attenuate PCS-mediated activation of the NF-κB/RUNX2 signaling pathway, suggesting that these agents demonstrate notable therapeutic potential for targeting PCS-induced CAVD.

*Correspondence to:* Dr Yi-Jen Chen, Graduate Institute of Clinical Medicine, College of Medicine, Taipei Medical University, 250 Wuxing Street, Xinyi, Taipei 110301, Taiwan, R.O.C.
E-mail: yjchen@tmu.edu.tw

*Key words:* p-cresol sulfate, klotho, calcific aortic valve disease, sirtuin-1, runt-related transcription factor 2, valvular interstitial cell

## Introduction

Calcific aortic valve disease (CAVD) is the most prevalent valvular heart disease. Aortic valve (AV) calcification causes restricted valve opening, leading to an unfavorable prognosis marked by complications, including congestive heart failure and sudden cardiac death. Therapeutic options for CAVD remain scarce despite its clinical importance due to the

poor elucidation of mechanisms underlying its pathogenesis. Currently, surgical or transcatheter AV replacement represent the only standard treatment strategies for CAVD. Notably, patients with chronic kidney disease (CKD) demonstrate a higher prevalence of CAVD (28-85%) and severe aortic stenosis (6-13%) than patients without CKD (1,2). CKD is characterized by the progressive loss of renal function, causing uremic toxin accumulation that contributes to cardiovascular complications. Among these toxins, p-cresyl sulfate (PCS), a gut microbiota-generated p-cresol-derived metabolite, has been implicated in kidney deterioration and cardiovascular diseases (3-5). Circulating PCS levels increase as renal function decreases (6); however, the role of PCS in CKD-induced valvular calcification remains ambiguous.

The klotho/sirtuin-1 (SIRT1) pathway has previously been implicated in the pathogenesis of renal-related diseases (7-11). SIRT1 upregulation has been associated with endoplasmic reticulum stress inhibition and vascular calcification attenuation in CKD (12). CKD progression is notably associated with klotho downregulation. Previous studies have demonstrated that uremic toxins promote klotho suppression and the upregulation of hypoxia-inducible factor-1α (HIF-1α) (13,14), a transcription factor that has been shown to be rapidly degraded within minutes under normoxic conditions via the ubiquitin-proteasome system (15). HIF-1α further suppresses klotho expression by activating p53 (16,17). These findings suggest that PCS, as a uremic toxin, can directly impact klotho/SIRT1 and HIF-1α signaling in valvular interstitial cells (VICs).

Klotho deficiency has been demonstrated to upregulate runt-related transcription factor 2 (RUNX2), a key driver of osteogenic gene transcription, in AVs. Furthermore, klotho deficiency has been shown to promote AV fibrosis, potentially via the AMP-activated protein kinase α/RUNX2 pathway (18). Recombinant klotho has been shown to attenuate hyperphosphatemia-induced osteogenic responses in human aortic VICs (19). Additionally, our previous study demonstrated that an osteogenic medium reduced klotho expression in aortic VICs (20), highlighting the important role of klotho in RUNX2 regulation. However, the role of klotho in CKD-associated CAVD remains to be fully elucidated.

SIRT1 activation has been demonstrated to mitigate klotho deficiency-induced vascular disease (21). In human calcified aortic stenosis, SIRT1 protein levels are reduced within AV leaflets (22). One study on aged apolipoprotein $E^{-/-}$ mice has demonstrated that resveratrol, a SIRT1 activator, inhibits AV calcification and AV stenosis progression (23). As an $NAD^+$-dependent class III deacetylase, SIRT1 regulates inflammation, cell death and metabolism through deacetylation (24,25). Furthermore, SRT1720, another SIRT1 activator, has been reported to reduce vascular smooth muscle cell calcification by inhibiting the RUNX2 pathway (26).

The present study aimed to investigate whether PCS directly enhanced VIC calcification, thus contributing towards CKD-associated CAVD, and aimed to explore the therapeutic potential of the klotho/SIRT1 pathway in VIC osteogenesis.

## Materials and methods

*Isolation and culture of porcine VICs.* As previously described (20), AV leaflets were obtained from 6-month-old pig hearts purchased from a commercial slaughterhouse (Yahsen Frozen Foods, Co., Ltd.). AVs were digested with collagenase I (250 U/ml; MilliporeSigma) for 30 min with gentle shaking at 37˚C to remove endothelial cells, and then were subjected to a second digestion for 12 h with collagenase I (250 U/ml) under gentle rocking at 37˚C to isolate VICs. As previously described, isolated VICs were cultured in a DMEM/F12 medium (MilliporeSigma) (20). The Institutional Animal Care and Use Committee (IACUC) of Taipei Medical University (Taipei, Taiwan) reviewed and approved the use of AV tissues and primary VICs in the present study (approval no. LAC 2020-0332).

*Induction of osteogenesis in aortic VICs and associated treatments.* Aortic VICs ($1x10^5$/well in the 6-well plate) were cultured in DMEM/F12 medium in a cell culture incubator at 37˚C for 7 days in the presence or absence of PCS (10 and 100 $\mu$M; APExBIO Technology LLC). The present study selected a PCS concentration of 100 $\mu$M to reflect the comparatively high PCS levels observed in advanced CKD (27). To clarify the underlying mechanism of PCS activity on VIC calcification, VICs were also incubated with PX-478 (0.5 $\mu$M; cat. no. HY-10231; MedChemExpress), recombinant klotho (100 pM; cat. no. APA798Hu02; Cloud-Clone Corp. CCC) and the SIRT1 activator SRT1720 (1 mM; cat. no. CAS 925434-55-5; Calbiochem; Merck KGaA) at 37˚C and refreshed every 24 h before further analysis.

*Calcification assessment.* Alizarin Red S (ARS) staining was performed in isolated VICs to visualize and quantify calcium deposition. VICs were fixed with 4% paraformaldehyde for 15 min and incubated with ARS staining solution for 1 h, both at room temperature. Subsequently, the excess dye was removed and the sample was washed with distilled water. ARS-stained cells were imaged using an Olympus CKX41 fluorescence microscope (Olympus Corporation). Calcification was subsequently quantified using ImageJ software (version 1.53t, National Institutes of Health).

*Western blot analysis.* Proteins extracted from aortic VICs were extracted using RIPA lysis buffer (MilliporeSigma) supplemented with protease and phosphatase inhibitors. Protein concentrations were determined using a BCA protein assay kit (Thermo Fisher Scientific, Inc.). Equal amounts of protein (30 $\mu$g per lane) were separated on 5-12% gradient gels using SDS-PAGE and transferred onto a PVDF membrane. The membranes were blocked with 10% non-fat milk in PBS for 1 h at room temperature and incubated overnight at 4˚C with primary antibodies against RUNX2 (1:2,000 dilution; cat. no. 12556; Cell Signaling Technology), acetylated-NF-κB (1:2,000 dilution; acetyl-NF-κB; cat. no. 3045; Cell Signaling Technology, Inc.), NF-κB (1:3,000 dilution; cat. no. 8242; Cell Signaling Technology, Inc.), HIF-1α (1:1,000 dilution; cat. no. NB100-479; Novus Biologicals), klotho (1:1,000 dilution; cat. no. LS-C145689; LifeSpan BioSciences, Inc.) and β-actin (1:6,600 dilution; cat. no. ab6276; Abcam). After washing, membranes were incubated with HRP-conjugated goat anti-rabbit IgG-HRP (cat. no. 7074; Cell Signaling Technology, Inc.) or goat anti-mouse IgG-HRP (cat. no. 7076; Cell Signaling Technology, Inc.) secondary antibodies for 1 h

at room temperature. Protein bands were visualized using an enhanced chemiluminescence kit (Thermo Fisher Scientific). Band intensities were quantified using ImageJ software (version 1.53, NIH) and normalized to β-actin.

*PCS-induced CKD rat model development and klotho recombinant protein administration*. Male Wistar rats aged 8 weeks (~250 g; n=13) were used in this study. The animals were obtained from BioLASCO Taiwan Co., Ltd. Prior to experimentation, the rats were allowed to acclimatize for at least 1 week under controlled housing conditions. Animals were maintained in a specific pathogen-free animal facility at a temperature of 19-21˚C with 40-70% relative humidity and a 12-h light/12-h dark cycle. Rats had *ad libitum* access to food and water, and were fed a standard laboratory diet (LabDiet® 5001; PMI Nutrition International). All animals were housed in standard cages under routine veterinary monitoring throughout the experimental period. The rats were divided into the following three groups: Control rats (n=4), PCS-induced CKD model rats (n=5) and PCS-induced CKD rats (n=4) treated with rat klotho recombinant protein (0.01 mg/kg/day; cat. no. RPH757Ra02; Arp Inc.). To induce the CKD model, rats were subject to intraperitoneal injection of PCS (50 mg/kg/day; APExBIO Technology LLC) for 4 weeks; rats were anesthetized with isoflurane prior to injections, which was administered by inhalation at a flow rate of 1 l/min (induction, 5%; maintenance, 2% with oxygen). The CKD control group was injected with the same volume of isotonic saline for the following 8 weeks. The CKD + klotho group also received 0.01 mg/kg klotho protein dissolved in 0.01 mol/l PBS via intraperitoneal injection once every 2 days for a total of 8 weeks following the 4-week PCS treatment. After 12 weeks, all rats were euthanized via administration of 5% isoflurane in oxygen until breathing had ceased. Upon observation of a loss of righting reflex and the absence of a response to a toe pinch, bilateral thoracotomy was performed as a secondary physical method of euthanasia to ensure that rats had been successfully sacrificed. Death was confirmed by auscultation to detect the cessation of respiration and the absence of a heartbeat for ≥5 min, as well as by confirmation of the absence of a corneal reflex. A bilateral thoracotomy was then performed and the heart tissue was extracted. The animal experiments performed in the present study were approved by the IACUC of Taipei Medical University (approval no. LAC 2023-0087).

*Immunohistochemistry (IHC)*. AVs isolated from rats were fixed in 4% paraformaldehyde and embedded in paraffin at room temperature for 2 h, followed by routine paraffin embedding. Paraffin-embedded tissues were sectioned at 3-$\mu$m thickness and mounted on FRC-13 slides (Matsunami Glass). Sections were deparaffinized in Surgipath xylene (cat. no. 3803665; Leica Biosystems) twice for 10 min each, and rehydrated through a descending ethanol series consisting of 100, 95, 80 and 70% Surgipath reagent alcohol (cat. no. 3803686; Leica Biosystems) for 5 min each, followed by washing in tap water for 5 min.

Heat-induced epitope retrieval was performed using citrate antigen retrieval buffer (cat. no. CBB500; Scytek Laboratories, Inc.) for 30 min, after which sections were washed with TBST wash buffer (cat. no. TBT999; Scytek Laboratories, Inc.) for 5 min. Endogenous peroxidase activity was blocked using Peroxidase Block (cat. no. RE7157; Novolink; Leica Biosystems) for 10 min at room temperature, followed by TBST washes twice for 3 min each. Non-specific binding was blocked using Protein Block solution (cat. no. RE7158; Novolink; Leica Biosystems) for 10 min at room temperature, followed by TBST washes twice for 3 min each.

Sections were incubated with a rabbit monoclonal anti-RUNX2 antibody (cat. no. 12556; Cell Signaling Technology, Inc.), diluted 1:30 in antibody dilution buffer (cat. no. ADB250; Roche Tissue Diagnostics), overnight at 4˚C in a humidified chamber. After primary antibody incubation, slides were washed with TBST twice for 3 min each. Signal detection was performed using the Polink-2 Plus HRP Rabbit DAB Kit [cat. no. D39-6; GBI (Labs) Ltd.] according to the manufacturer's instructions. Briefly, sections were incubated with Rabbit Antibody Enhancer for 15 min at room temperature, washed with TBST twice for 3 min, and subsequently incubated with Polymer-HRP for Rabbit for 15 min at room temperature.

Immunoreactivity was visualized using DAB chromogen (cat. no. RE7270-K; Novolink; Lecia Biosystems) for 5 min at room temperature. Slides were rinsed in tap water for 5 min, counterstained with Surgipath Hematoxylin Gill II (cat. no. 3801522; Leica Biosystems) for 5 min and washed again in tap water for 5 min. Sections were then dehydrated in 100% ethanol twice for 5 min each, cleared in xylene twice for 5 min each, and mounted using Surgipath Micromount mounting medium (cat. no. 3801731; Leica Biosystems). RUNX2 expression was quantified using ImageJ (version 1.53t, National Institutes of Health) under an Olympus CKX41 fluorescence microscope (Olympus Corporation).

*Statistical analysis*. All parameters are expressed as the mean ± SEM. Statistical analyses were performed using unpaired Student's t-test between two groups or one-way analysis of variance for multiple groups. Post-hoc analysis was performed using Tukey's multiple comparisons test. Statistical analyses were performed using Graphpad Prism 9 (Dotmatics). $P<0.05$ was considered to indicate a statistically significant difference.

## Results

*Effects of PCS on VIC calcification*. The present study incubated VICs with 10 and 100 $\mu$M PCS to investigate the effect of PCS on VIC calcification, as well as its impact on RUNX2 expression. The present study observed that, compared with untreated VICs, incubation with 100 $\mu$M PCS significantly increased VIC calcification (Fig. 1A) and RUNX2 protein expression (Fig. 1B). Furthermore, treatment with PCS significantly decreased klotho expression and significantly increased HIF-1α expression in VICs (Fig. 2).

*Effects of a HIF-1α inhibitor, recombinant klotho and SIRT1 activator on VIC calcification*. The present study investigated whether HIF-1α or klotho modulated the effects of PCS in VICs. Treatment with the HIF-1α inhibitor PX-478 (0.5 $\mu$M) was shown to significantly reduce PCS-mediated calcification of VICs (Fig. 3). Additionally, klotho (100 pM) administration significantly attenuated PCS-induced calcification by 24.4% (Fig. 4). Furthermore, klotho administration significantly

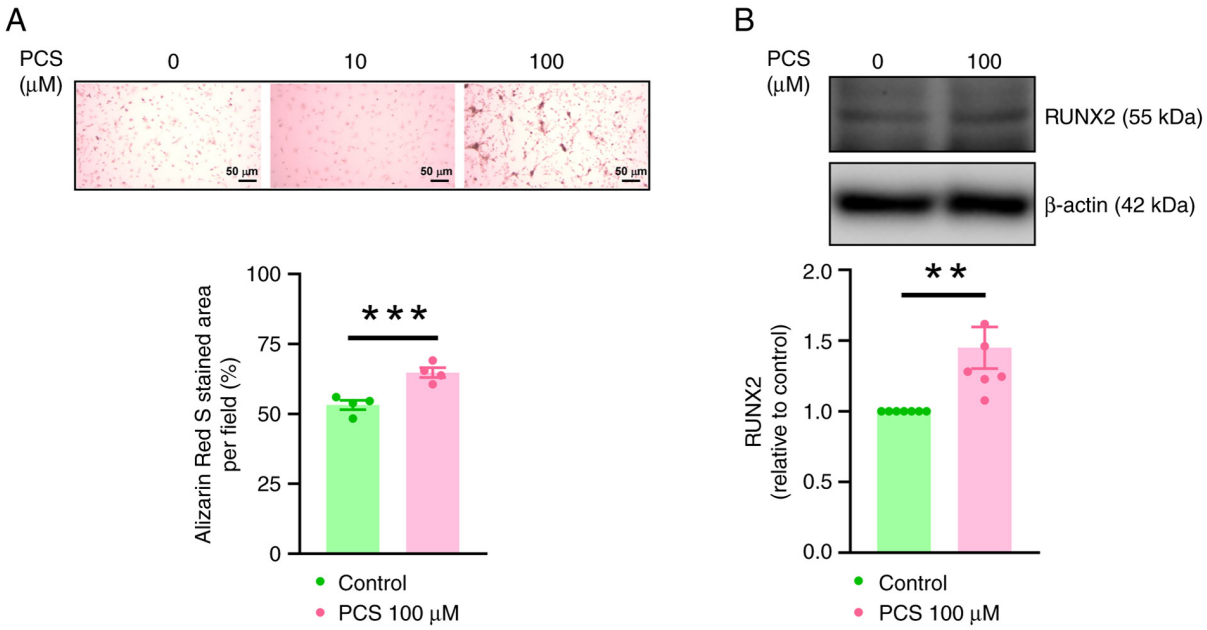


Figure 1. Effect of PCS on VIC calcification. (A) The upper panel contains representative images of Alizarin Red S-stained VICs that were cultured with various concentrations of PCS. VIC calcification was quantified by determining the total area of positive staining (red) per field (3 fields were observed per treatment group), as shown in the lower panel (n=6). Scale bar, 50 $\mu$m. (B) Western blotting and semi-quantification of RUNX2 protein expression in control and PCS-treated VICs (n=7). β-actin was used as an internal control. $^{**}$P<0.01 and $^{***}$P<0.005. PCS, p-cresol; RUNX2, runt-related transcription factor 2; VIC, valvular interstitial cell.

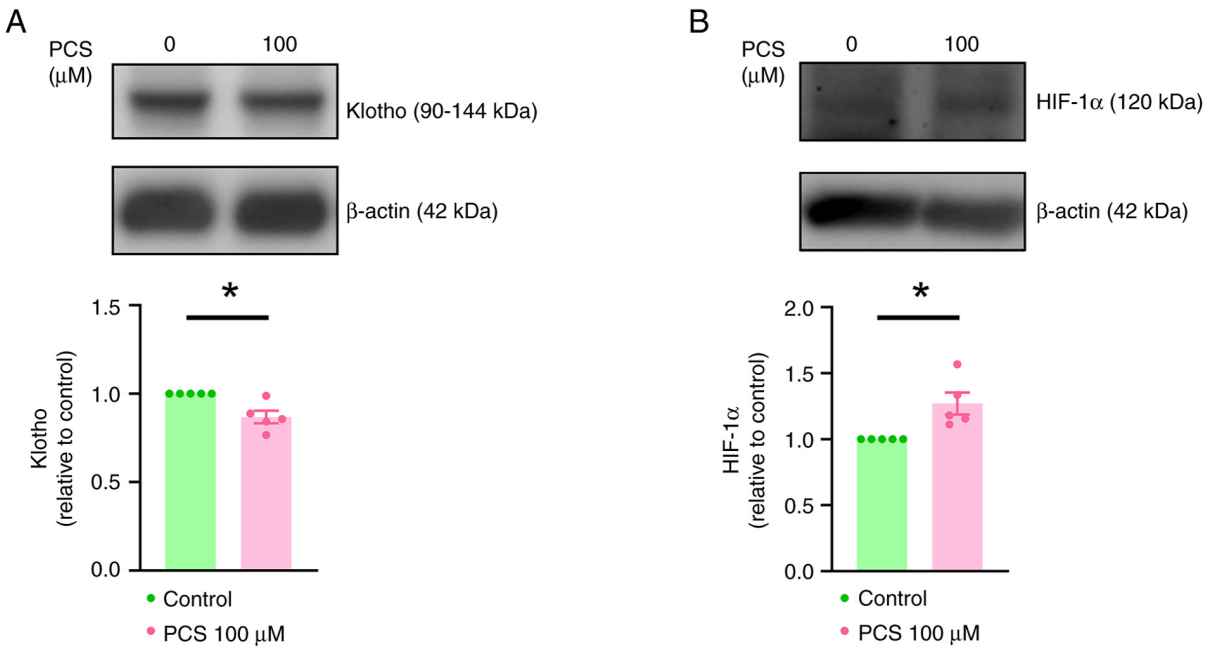


Figure 2. Effect of PCS on klotho and HIF-1α expression. Western blotting and semi-quantification of (A) klotho and (B) HIF-1α protein expression in control and PCS-treated valvular interstitial cells. PCS-treated cells were incubated with PCS (100 $\mu$M) for 7 days (n=5). β-actin was used as an internal control. $^{*}$P<0.05. PCS, p-cresol; HIF-1α, hypoxia-inducible factor-1α.

attenuated PCS-induced increases in the expression levels of RUNX2 and acetyl-NF-κB/total NF-κB in VICs (Fig. 5).

Similarly, the present study examined the effects of SIRT1 on PCS-treated VICs. ARS staining revealed that SRT1720 (1 mM), a SIRT1 activator, significantly reduced PCS-induced VIC calcification (Fig. 6). Furthermore, SRT1720 significantly attenuated PCS-mediated downregulation of klotho and significantly reduced PCS-enhanced RUNX2 expression in VICs (Fig. 7). PCS administration also resulted in the elevation of NF-kB acetylation compared with the control group, which was significantly mitigated by co-treatment with klotho. These findings suggested that activation of the klotho/SIRT1 axis was important for preventing PCS-induced VIC calcification.

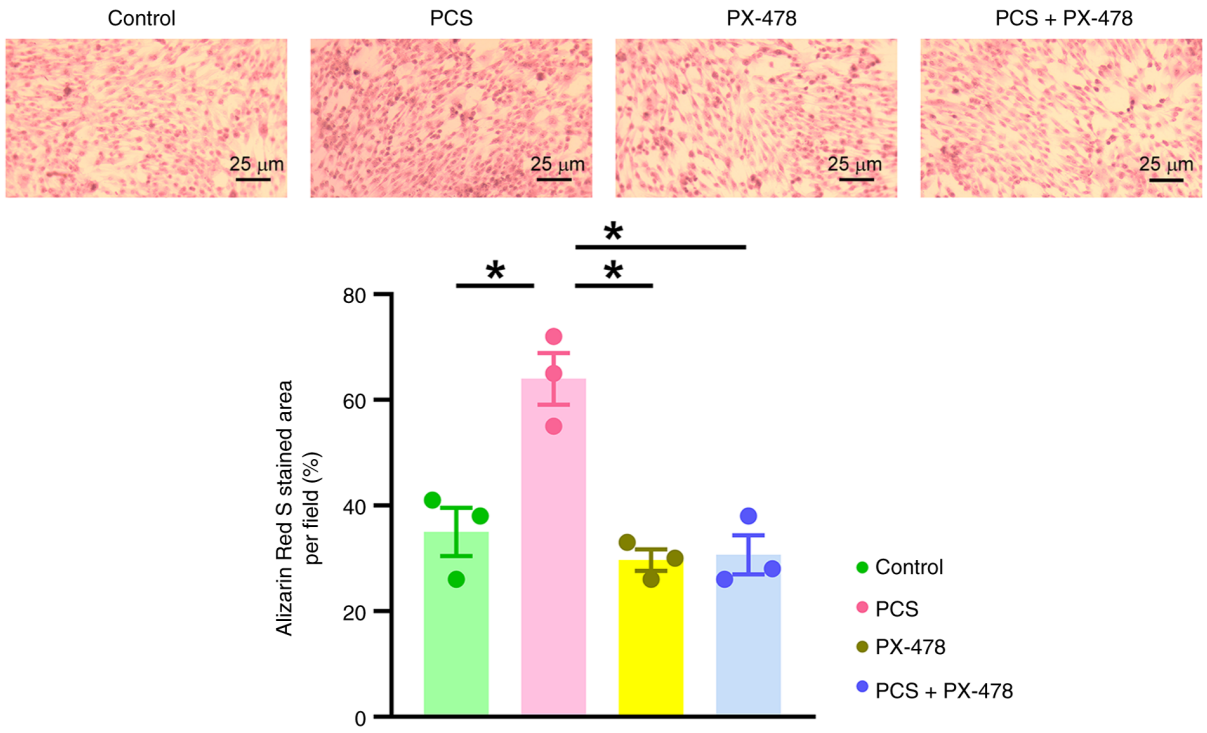


Figure 3. Effect of HIF-1α inhibition on PCS-induced VIC calcification. The upper panel depicts representative images of Alizarin Red S-stained VICs that have been incubated with or without the HIF-1α inhibitor PX-478 (0.5 $\mu$M) and with or without PCS (100 $\mu$M). VIC calcification was quantified by determining the total area of positive staining (red) per field (3 fields were observed per treatment group), as shown in the lower panel (n=3). Scale bar, 25 $\mu$m. *P<0.05. PCS, p-cresol; VIC, valvular interstitial cell; HIF-1α, hypoxia-inducible factor-1α.

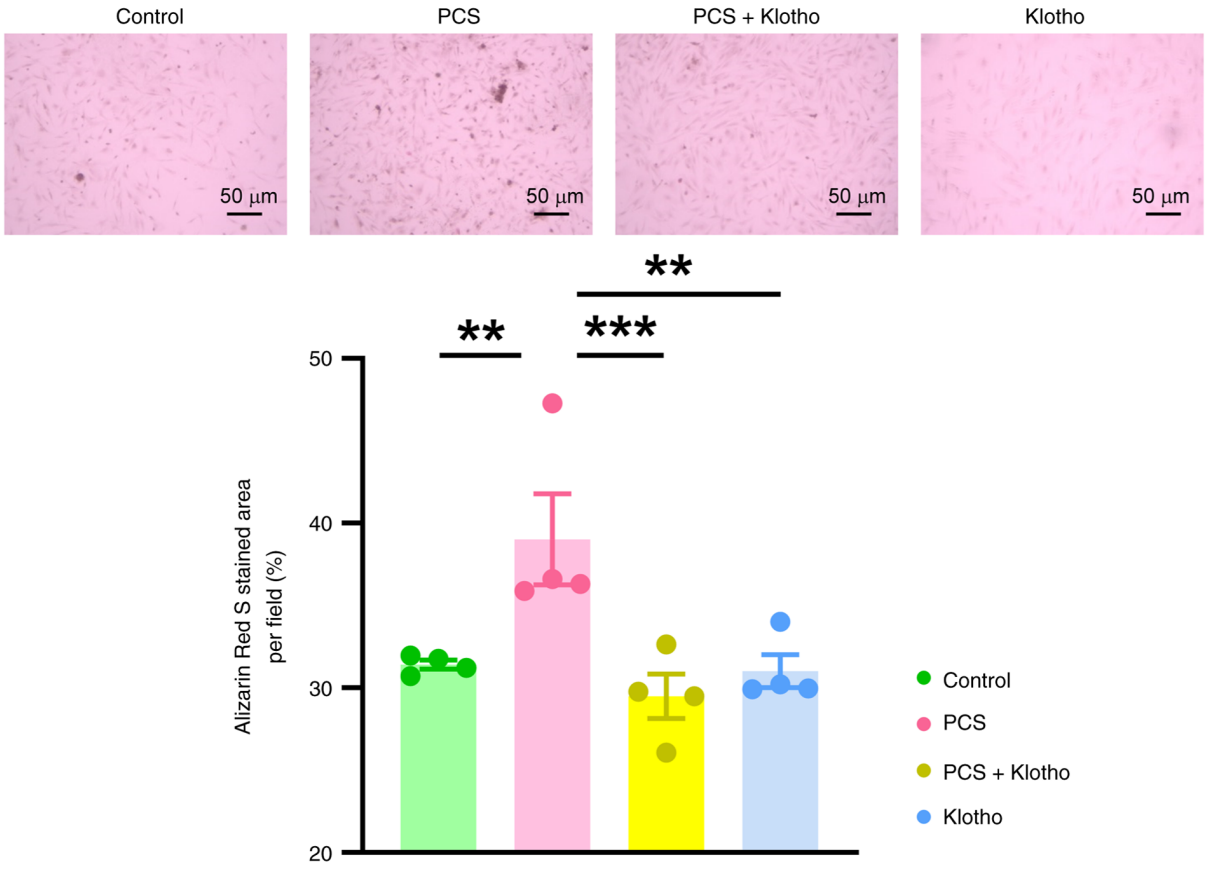


Figure 4. Effect of recombinant klotho on PCS-induced VIC calcification. The upper panel depicts representative images of Alizarin Red S-stained VICs incubated with or without klotho (100 pM) and with or without PCS (100 $\mu$M). VIC calcification was quantified by determining the total area of positive staining (red) per field (3 fields were observed per treatment group), as shown in the lower panel (n=4). Scale bar, 50 $\mu$m. **P<0.01 and ***P<0.005. PCS, p-cresol; VIC, valvular interstitial cell.

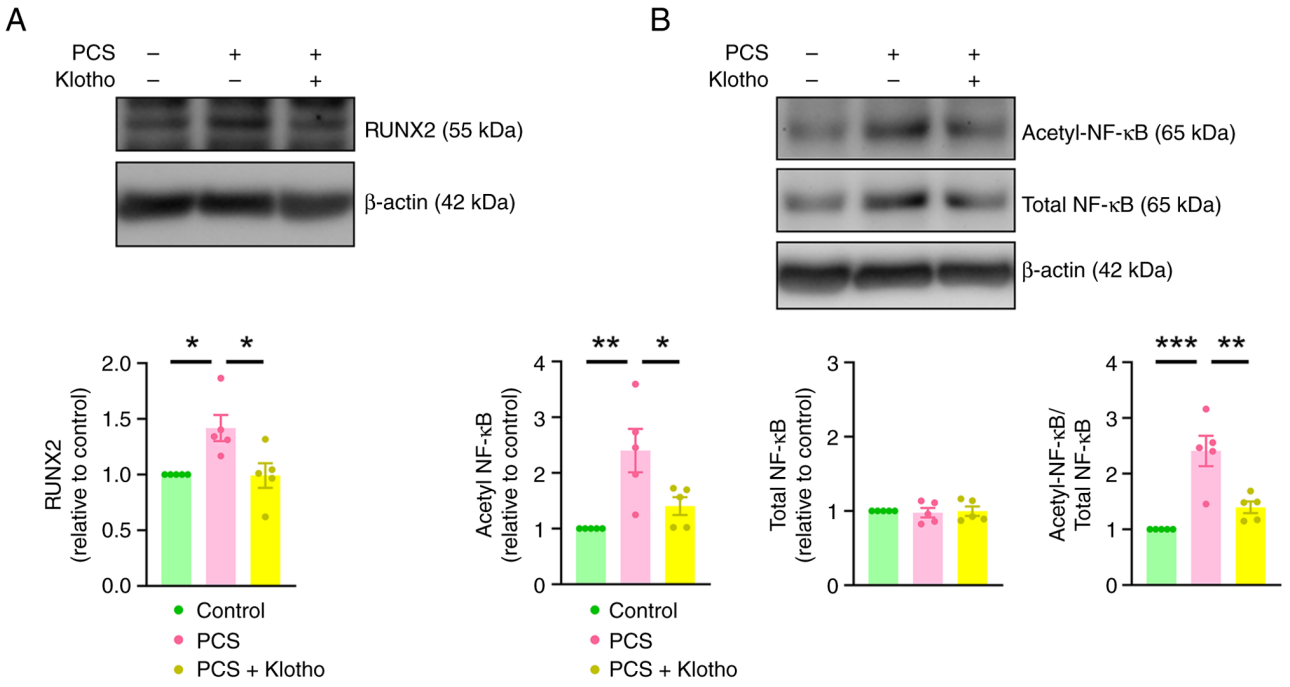


Figure 5. Effect of klotho supplementation on PCS-mediated upregulation of RUNX2 and NF-kB acetylation in valvular interstitial cells. Western blotting and semi-quantification of (A) RUNX2 expression and (B) NF-kB acetylation in control cells, cells treated with PCS and cells treated with PCS + klotho (n=5). β-actin was used as an internal control. *P<0.05, **P<0.01 and ***P<0.005. PCS, p-cresol; RUNX2, runt-related transcription factor 2; acetyl-NF-κB, acetylated-NF-κB.

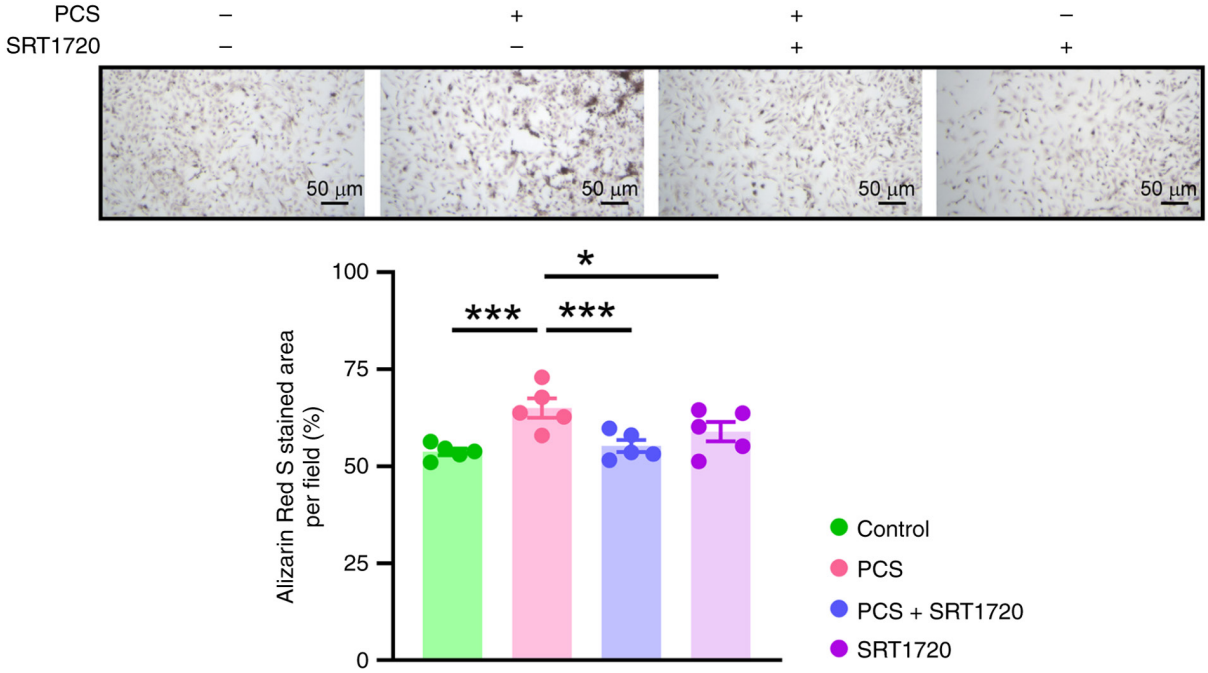


Figure 6. Effect of SRT1720 on PCS-induced VIC calcification. The upper panel depicts representative images of Alizarin Red S-stained VICs incubated with or without SRT1720 (1 mM) and with or without PCS (100 $\mu$M). VIC calcification was quantified by determining the total area of positive staining (red) per field, as shown in the lower panel (n=4); 3 fields were observed per treatment group. Scale bar, 50 $\mu$m. *P<0.05 and ***P<0.005. PCS, p-cresol; VIC, valvular interstitial cell.

*Klotho ameliorates CKD-mediated RUNX2 upregulation in PCS-treated AVs*. The present study developed a PCS-induced rat model of CKD to evaluate whether klotho played a role in the CKD-mediated upregulation of RUNX2. Rats were treated with recombinant klotho protein for a total of 8 weeks. IHC revealed that PCS-induced CKD model rats exhibited a significant increase in RUNX2 expression in the AV leaflet (Fig. 8). Treatment with recombinant klotho mitigated the CKD-mediated upregulation of RUNX2 in PCS-induced model rats.

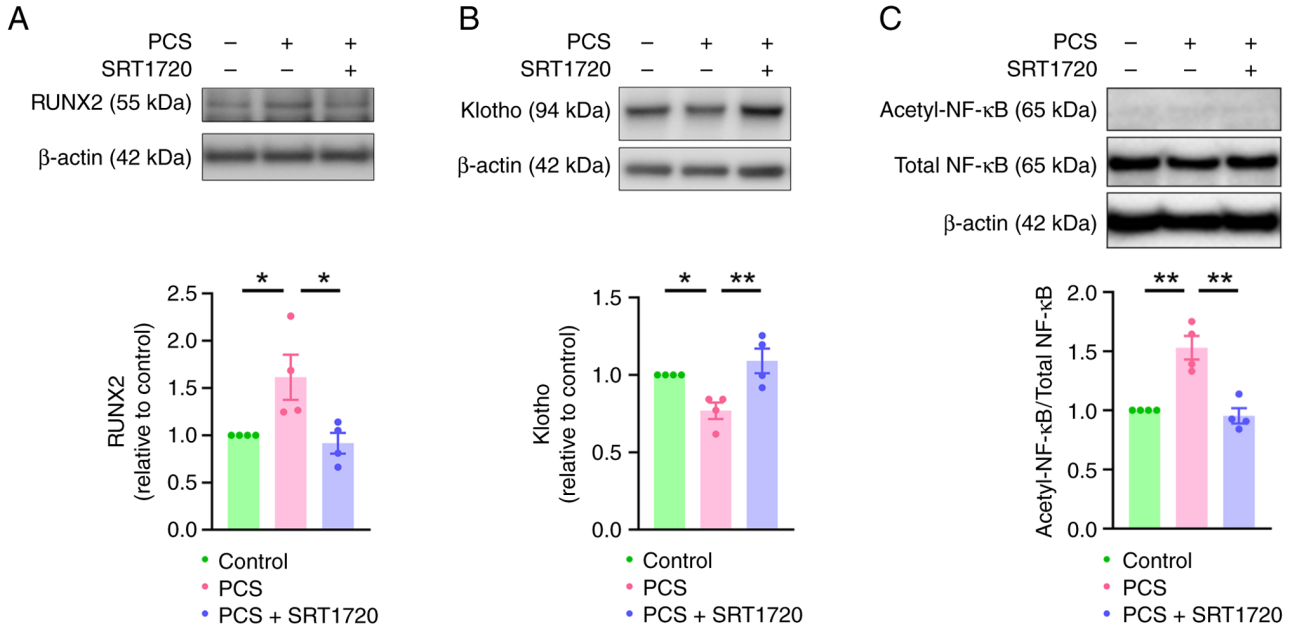


Figure 7. Effect of sirtuin-1 activation on klotho and RUNX2 expression. (A) Representative western blots demonstrating the effect of SRT1720 (1 mM) treatment on RUNX2 protein expression in PCS-treated VICs, compared with untreated controls and VICs treated with PCS alone. RUNX2 expression was semi-quantified in each group for statistical comparisons between groups (n=6). (B) Representative western blots demonstrating the effect of SRT1720 on klotho protein expression in PCS-treated VICs, compared with untreated controls and VICs treated with PCS alone. Klotho expression was semi-quantified in each group for statistical comparisons between groups (n=6). (C) Representative western blots demonstrating the effect of SRT1720 on acetyl-NF-kB and total NF-kB protein expression in PCS-treated VICs, compared with untreated controls and VICs treated with PCS alone. NF-kB and acetyl-NF-kB expression levels were semi-quantified in each group for statistical comparisons between groups (n=8). $^{*}$P<0.05 and $^{**}$P<0.01. PCS, p-cresol; RUNX2, runt-related transcription factor 2; acetyl-NF-κB, acetylated-NF-κB; VIC, valvular interstitial cell.

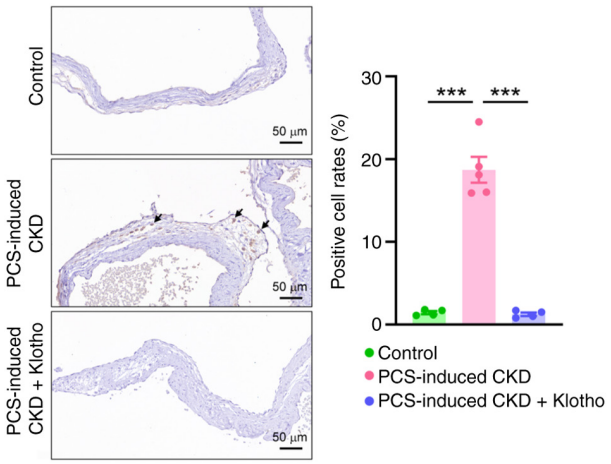


Figure 8. Effect of klotho on RUNX2 expression in the aortic valves of PCS-induced CKD model rats. Representative immunohistochemistry images displaying RUNX2 expression in rat aortic valves in control (n=4), PCS-induced CKD (n=5) and PCS-induced CKD + klotho rats (n=4). Scale bar, 50 $\mu$m. Immunohistochemical results were quantified to statistically compare RUNX2 expression between treatment groups by % of positive staining. The arrows within the IHC images in this figure indicate the RUNX2 expression. $^{***}$P<0.005. PCS, p-cresol; CKD, chronic kidney disease; RUNX2, runt-related transcription factor 2.

## Discussion

Elevated levels of circulating PCS have previously been associated with an increased risk of cardiovascular disease in patients with CKD (22). Furthermore, CKD occurrence is associated with increased HIF-1α expression (28-30). PCS, a uremic toxin, is associated with the pathogenesis of arterial stiffness in CKD (31). A PCS concentration of 100 $\mu$M was used in the *in vitro* protocols of the present study in order to reflect the high physiological levels of PCS observed in CKD. The high physiological levels of PCS in CKD have been suggested to promote cellular stress, contributing to conditions such as AV stenosis (32). To the best of our knowledge, the present study demonstrated for the first time that PCS upregulated HIF-1α expression levels in VICs. Previous studies have demonstrated that HIF-1α upregulates RUNX2 expression in stem cells by activating vascular endothelial growth factor (33), which may further contribute to RUNX2 upregulation in VICs (34). The results of the present study indicated that inhibition of HIF-1α activity significantly ameliorated PCS-mediated calcification of VICs.

In patients with end-stage kidney disease, plasma PCS concentrations have been reported to range from 115 to >500 $\mu$M, whereas healthy individuals demonstrate concentration levels of 15-35 $\mu$M (35). In the VIC culture system used in the present study, 100 $\mu$M PCS was selected for CKD modelling as it was considered within the upper pathophysiological range of serum PCS concentrations observed in advanced CKD, and this aligned with PCS concentrations used in a previous *in vitro* study of PCS-induced toxicity in vascular and renal cells, which typically range from 20-500 $\mu$M (36).

Furthermore, the results of the present study revealed that PCS administration reduced klotho expression and increased HIF-1α expression, which suggested that this effect may be mediated by upregulating HIF-1α. Mechanistically, a previous study has established that HIF-1α-dependent p53 activation suppresses klotho expression (17). Under hypoxic conditions

(low oxygen availability), HIF-1α is stabilized and translocates into the nucleus. HIF-1α activation has been shown to suppress klotho activity by inducing the expression of microRNAs (miRs), such as miR-34a, and other mediators that reduce klotho levels, fostering a feedback loop associating oxygen availability, klotho and HIF-1α (33). Although no knockdown experiments were performed in the present study to isolate this specific pathway, existing literature and parallel observations in our previous study strongly support this mechanism (34). Specifically, PCS treatment simultaneously upregulated HIF-1α and downregulated klotho, whereas klotho supplementation was shown to decrease the osteogenic phenotype. These findings suggested that the PCS-induced simultaneous upregulation of HIF-1α and suppressed klotho expression resulted in the observed calcification of VICs.

The observed attenuation of PCS-induced VIC calcification resulting from klotho supplementation suggested that PCS-mediated klotho downregulation significantly promoted VIC calcification. Consistent with the results of a previous study (37), the present study also demonstrated reduced klotho with increased HIF-1α in VICs. Klotho deficiency may contribute, at least in part, to the HIF-1α activation. The *in vivo* experiments of the present study revealed that klotho administration reduced PCS-mediated upregulation of RUNX2 in the AVs of CKD model rats. The present study focused on the effects of PCS on the expression of RUNX2, which is an important driver of osteogenic transdifferentiation in AVs. The present study identified that, in CKD model rats that were treated with PCS for 4 weeks, PCS upregulated RUNX2 expression in rat AVs; however, no calcium deposition was detected via the Alizarin red S staining. This result likely reflects the model's relatively early stage, as CKD-associated metabolic disturbances often precede overt mineral deposition. The results of the present study also demonstrated that klotho supplementation mitigated the PCS-induced upregulation of RUNX2 in the AVs of rats. Accordingly, future studies should analyze a broader panel of histological markers, such as HIF-1α or klotho, and extend the duration of CKD model induction.

Furthermore, klotho deficiency has been demonstrated to aggravate inflammation by activating the NF-κB/RUNX2 axis (38,39). Given that NF-κB activation is a key driver of CAVD pathogenesis (39), klotho has been shown to play a protective role by preventing NF-κB nuclear translocation and reducing its transcriptional activity (26). Soluble klotho administration in klotho-mutant mice and membrane-bound klotho overexpression in cultured cells have been shown to suppress NF-κB signaling and its downstream effects (40). Our previous study also demonstrated that the incubation of aortic VICs in an osteogenic culture medium reduced klotho expression (20). Furthermore, PCS has been reported to reduce klotho expression in renal tubules by inducing klotho gene hypermethylation (13). Previous findings have further suggested that klotho can mitigate the deleterious effects of PCS on the heart (35). Collectively, these findings have provided substantial evidence that the PCS/NF-κB/RUNX2 axis markedly contributes to klotho suppression and VIC calcification. Notably, the present study demonstrated that klotho supplementation attenuated PCS-induced VIC calcification, highlighting the important role of klotho deficiency in both *in vivo* (CKD-induced) and *in vitro* (PCS-induced) settings. The results of the present study suggested that PCS significantly contributed to AV calcification in CKD.

A previous study has demonstrated that klotho deficiency inhibits SIRT1 activity and that pharmacological activation of SIRT1 with SRT1720 can ameliorate klotho deficiency-induced arterial stiffness (21). Furthermore, SRT1720 has been demonstrated to suppress HIF-1α expression both *in vivo* and *in vitro* (41). A study by Szymanska *et al* (42) reported that treatment with resveratrol or SRT2104, a SIRT1-specific activator, notably decreased HIF-1α levels. Additionally, SIRT1-mediated deacetylation of HIF-1α has been shown to inhibit its transcriptional activity (43). As such, SRT1720 may have enhanced klotho expression and mitigated PCS-induced VIC calcification by suppressing HIF-1α. The findings of the present study suggested that klotho supplementation and SIRT1 activation attenuated the pro-calcific effects of PCS on VICs. The present study also demonstrated that SRT1720 treatment inhibited RUNX2 expression in PCS-treated VICs, indicating that SIRT1 demonstrated a regulatory role in valvular calcification. Therefore, SIRT1 signaling activation may represent a promising therapeutic strategy for mitigating PCS-enhanced CAVD.

Considering that the surgical or transcatheter replacement of AVs remain the standard treatment strategies for CAVD, the results of the present study support the feasibility of the klotho/SIRT1 axis as a target for CAVD treatment, and suggest that this pathway represents an important avenue for future clinical translation. Therapeutic strategies aimed at restoring klotho expression or enhancing SIRT1 activity therefore represent potential approaches for mitigating CKD-associated CAVD. Recombinant klotho protein, genetic or small-oligonucleotide-based klotho upregulation strategies (44) and pharmacological SIRT1 activators, for example resveratrol analogs and SRT1720 derivatives, are currently under preclinical evaluation for use in CAVD-targeting therapies; these strategies could, in principle, be combined with PCS-lowering interventions, such as gut microbiota modulation, protein-bound uremic toxin binders or optimized dialysis modalities, to reduce valvular exposure to uremic toxins. The findings of the present study offered mechanistic insights for future translational studies targeting the klotho/SIRT1 axis for decreasing PCS burden in patients with both CKD and CAVD.

In conclusion, the uremic toxin PCS induced VIC calcification via HIF-1α/RUNX2 signaling pathway activation and concurrent klotho downregulation. Activation of the klotho/SIRT1 pathway, via recombinant klotho or SRT1720, effectively attenuated PCS-induced VIC calcification and may represent a potential therapeutic strategy for mitigating CAVD progression in CKD.

**Acknowledgements**

Not applicable.

**Funding**

The present study was funded by grants from Wan Fang Hospital (grant nos. 107TMU-WFH-01-1, 108TMU-WFH-01-3, 110-eva-24, 111-wf-eva-30, 112-wf-eva-17 and 113-wf-eva-38),

Taipei Medical University (grant no. TMU109-AE1-B09) and the National Science and Technology Council, Taiwan, R.O.C. (grant nos. MOST108-2314-B-038-120 and NSTC 112-2314-B-038-107).

## Authors' contributions

SL, YK, NT, PC and YC were responsible for the conceptualization of the present study. SL, WC, CC and TC analyzed the data in the present study. SL, TC, WC and NT were responsible for reviewing/investigation of existing research on the topics discussed in the study. TC, NT, PC and YC were responsible for the design of the methods used in the study. SL and TC were responsible for the acquisition of materials used in the present study. SL, TC and YC confirm the authenticity of all the raw data. SL and TC were also responsible for writing the initial draft of the manuscript. TC, YK, WC, CC, NT, PC and YC all contributed to reviewing and editing the manuscript. All authors have read and approved the final version of the manuscript.

## Ethics approval and consent to participate

The present study was approved by the Institutional Animal Care and Use Committee of Taipei Medical University (approval nos. LAC 2020-0332 and LAC 2023-0087).

## Patient consent for publication

Not applicable.

## Competing interests

The authors declare that they have no competing interests.

## References

1. Ikee R, Honda K, Ishioka K, Oka M, Maesato K, Moriya H, Hidaka S, Ohtake T and Kobayashi S: Differences in associated factors between aortic and mitral valve calcification in hemodialysis. Hypertens Res 33: 622-626, 2010.
2. Guerraty MA, Chai B, Hsu JY, Ojo AO, Gao Y, Yang W, Keane MG, Budoff MJ and Mohler ER III; CRIC Study Investigators: Relation of aortic valve calcium to chronic kidney disease (from the Chronic Renal Insufficiency Cohort Study). Am J Cardiol 115: 1281-1286, 2015.
3. Barreto FC, Barreto DV, Liabeuf S, Meert N, Glorieux G, Temmar M, Choukroun G, Vanholder R and Massy ZA; European Uremic Toxin Work Group (EUTox): Serum indoxyl sulfate is associated with vascular disease and mortality in chronic kidney disease patients. Clin J Am Soc Nephrol 4: 1551-1558, 2009.
4. Chiu CA, Lu LF, Yu TH, Hung WC, Chung FM, Tsai IT, Yang CY, Hsu CC, Lu YC, Wang CP and Lee YJ: Increased levels of total P-Cresylsulphate and indoxyl sulphate are associated with coronary artery disease in patients with diabetic nephropathy. Rev Diabet Stud 7: 275-284, 2010.
5. Liabeuf S, Barreto DV, Barreto FC, Meert N, Glorieux G, Schepers E, Temmar M, Choukroun G, Vanholder R and Massy ZA; European Uraemic Toxin Work Group (EUTox): Free p-cresylsulphate is a predictor of mortality in patients at different stages of chronic kidney disease. Nephrol Dial Transplant. 2010;25: 1183-1191, 2010.
6. Viaene L, Meijers BK, Bammens B, Vanrenterghem Y and Evenepoel P: Serum concentrations of p-cresyl sulfate and indoxyl sulfate, but not inflammatory markers, increase in incident peritoneal dialysis patients in parallel with loss of residual renal function. Perit Dial Int 34: 71-78, 2014.
7. Su H, Gao D, Chen Y and Zuo Z: The relationship between klotho and SIRT1 expression in renal aging related disease. Int J Gen Med 15: 7885-7893, 2022.
8. Hu MC, Kuro-o M and Moe OW: Klotho and chronic kidney disease. Contrib Nephrol 180: 47-63, 2013.
9. Giachelli CM: The emerging role of phosphate in vascular calcification. Kidney Int 75: 890-897, 2009.
10. Lindberg K, Amin R, Moe OW, Hu MC, Erben RG, Ostman Wernerson A, Lanske B, Olauson H and Larsson TE: The kidney is the principal organ mediating klotho effects. J Am Soc Nephrol 25: 2169-2175, 2014.
11. Hu MC, Shi M, Zhang J, Quinones H, Griffith C, Kuro-o M and Moe OW: Klotho deficiency causes vascular calcification in chronic kidney disease. J Am Soc Nephrol 22: 124-136, 2011.
12. Yan J, Wang J, He JC and Zhong Y: Sirtuin 1 in chronic kidney disease and therapeutic potential of targeting Sirtuin 1. Front Endocrinol (Lausanne) 13: 917773, 2022.
13. Sun CY, Chang SC and Wu MS: Suppression of Klotho expression by protein-bound uremic toxins is associated with increased DNA methyltransferase expression and DNA hypermethylation. Kidney Int 81: 640-650, 2012.
14. Liu H, Li Y and Xiong J: The role of hypoxia-inducible factor-1 alpha in renal disease. Molecules 27: 7318, 2022.
15. Marxsen JH, Stengel P, Doege K, Heikkinen P, Jokilehto T, Wagner T, Jelkmann W, Jaakkola P and Metzen E: Hypoxia-inducible factor-1 (HIF-1) promotes its degradation by induction of HIF-alpha-prolyl-4-hydroxylases. Biochem J 381 (Pt 3): 761-767, 2004.
16. Wu TK, Wei CW, Pan YR, Hsu RJ, Wu CY and Yu YL: The uremic toxin p-cresyl sulfate induces proliferation and migration of clear cell renal cell carcinoma via microRNA-21/HIF-1α axis signals. Sci Rep 9: 3207, 2019.
17. Xie L, Wang Y, Li Q, Ji X, Tu Y, Du S, Lou H, Zeng X, Zhu L, Zhang J and Zhu M: The HIF-1α/p53/miRNA-34a/Klotho axis in retinal pigment epithelial cells promotes subretinal fibrosis and exacerbates choroidal neovascularization. J Cell Mol Med 25; 1700-1711, 2021.
18. Chen J, Lin Y and Sun Z: Deficiency in the anti-aging gene Klotho promotes aortic valve fibrosis through AMPKalpha-mediated activation of RUNX2. Aging Cell 15: 853-860, 2016.
19. Li F, Yao Q, Ao L, Cleveland JC Jr, Dong N, Fullerton DA and Meng X: Klotho suppresses high phosphate-induced osteogenic responses in human aortic valve interstitial cells through inhibition of Sox9. J Mol Med (Berl) 95: 739-751, 2017.
20. Li SJ, Kao YH, Chung CC, Chen WY, Cheng WL and Chen YJ: Activated p300 acetyltransferase activity modulates aortic valvular calcification with osteogenic transdifferentiation and downregulation of Klotho. Int J Cardiol 232: 271-279, 2017.
21. Gao D, Zuo Z, Tian J, Ali Q, Lin Y, Lei H and Sun Z: Activation of SIRT1 attenuates klotho deficiency-induced arterial stiffness and hypertension by enhancing AMP-activated protein kinase activity. Hypertension 68: 1191-1199, 2016.
22. Carter S, Miard S, Roy-Bellavance C, Boivin L, Li Z, Pibarot P, Mathieu P and Picard F: Sirt1 inhibits resistin expression in aortic stenosis. PLoS One 7: e35110, 2012.
23. Cai Z, Wang J, Liu M, Yuan T and Li F: Abstract 12300: Sirtuin 1 Prevents Age-associated Aortic Valve Calcification in vivo. Circulation 140 (Suppl 1): A12300, 2019.
24. Lu C, Zhao H, Liu Y, Yang Z, Yao H, Liu T, Gou T, Wang L, Zhang J, Tian Y, *et al*: Novel Role of the SIRT1 in endocrine and metabolic diseases. Int J Biol Sci 19: 484-501, 2023.
25. Liu TF and McCall CE: Deacetylation by SIRT1 reprograms inflammation and cancer. Genes Cancer 4: 135-147, 2013.
26. Bartoli-Leonard F, Wilkinson FL, Schiro A, Inglott FS, Alexander MY and Weston R: Suppression of SIRT1 in diabetic conditions induces osteogenic differentiation of human vascular smooth muscle cells via RUNX2 signalling. Sci Rep 9: 878, 2019.
27. Poesen R, Viaene L, Verbeke K, Augustijns P, Bammens B, Claes K, Kuypers D, Evenepoel P and Meijers B: Cardiovascular disease relates to intestinal uptake of p-cresol in patients with chronic kidney disease. BMC Nephrol 15: 87, 2014.
28. Fu Q, Colgan SP and Shelley CS: Hypoxia: The force that drives chronic kidney disease. Clin Med Res 14: 15-39, 2016.
29. Hirakawa Y, Tanaka T and Nangaku M: Renal hypoxia in CKD; Pathophysiology and detecting methods. Front Physiol 8: 99, 2017.
30. Liu M, Ning X, Li R, Yang Z, Yang X, Sun S and Qian Q: Signalling pathways involved in hypoxia-induced renal fibrosis. J Cell Mol Med 21: 1248-1259, 2017.

31. Chern YB, Chia KL, Liu CH, Lin YL, Tsai JP and Hsu BG: Serum p-Cresyl sulfate is independently associated with aortic stiffness in non-dialysis chronic kidney disease patients. Life (Basel) 15: 1116, 2025.
32. Zoccali C, Mallamaci F, Adamczak M, de Oliveira RB, Massy ZA, Sarafidis P, Agarwal R, Mark PB, Kotanko P, Ferro CJ, *et al*: Cardiovascular complications in chronic kidney disease: A review from the European renal and cardiovascular medicine working group of the European renal association. Cardiovasc Res 119: 2017-2032, 2023.
33. Xu Q, Liu Z, Guo L, Liu R, Li R, Chu X, Yang J, Luo J, Chen F and Deng M: Hypoxia mediates runt-related transcription factor 2 expression via induction of vascular endothelial growth factor in periodontal ligament stem cells. Mol Cells 42: 763-772, 2019.
34. Li SJ, Kao YH, Chung CC, Cheng WL, Lin YK and Chen YJ: Vascular endothelial growth factor on Runt-related transcript factor-2 in aortic valve cells. Eur J Clin Invest 51: e13470, 2021.
35. Gryp T, Vanholder R, Vaneechoutte M and Glorieux G: p-Cresyl Sulfate. Toxins (Basel) 9: 52, 2017.
36. Watanabe H, Miyamoto Y, Enoki Y, Ishima Y, Kadowaki D, Kotani S, Nakajima M, Tanaka M, Matsushita K, Mori Y, *et al*: p-Cresyl sulfate, a uremic toxin, causes vascular endothelial and smooth muscle cell damages by inducing oxidative stress. Pharmacol Res Perspect 3: e00092, 2015.
37. Afsar B, Kanbay M and Afsar RE: Interconnections of fibroblast growth factor 23 and klotho with erythropoietin and hypoxia-inducible factor. Mol Cell Biochem 477: 1973-1985, 2022.
38. He T, Xiong J, Huang Y, Zheng C, Liu Y, Bi X, Liu C, Han W, Yang K, Xiao T, *et al*: Klotho restrain RIG-1/NF-κB signaling activation and monocyte inflammatory factor release under uremic condition. Life Sci 231: 116570, 2019.
39. Liu T, Zhang L, Joo D and Sun SC: NF-κB signaling in inflammation. Signal Transduct Target Ther 2: 17023-, 2017.
40. Zhao Y, Banerjee S, Dey N, LeJeune WS, Sarkar PS, Brobey R, Rosenblatt KP, Tilton RG and Choudhary S: Klotho depletion contributes to increased inflammation in kidney of the db/db mouse model of diabetes via RelA (serine)536 phosphorylation. Diabetes 60: 1907-1916, 2011.
41. Han W, Wang C, Yang Z, Mu L, Wu M, Chen N, Du C, Duan H and Shi Y: SRT1720 retards renal fibrosis via inhibition of HIF1A/GLUT1 in diabetic nephropathy. J Endocrinol 241: 85-98, 2019.
42. Szymanska M, Manthe S, Shrestha K, Girsh E, Harlev A, Kisliouk T and Meidan R: Sirtuin-1 inhibits endothelin-2 expression in human granulosa-lutein cells via hypoxia inducible factor 1 alpha and epigenetic modifications †. Biol Reprod 104: 387-398, 2021.
43. Ryu DR, Yu MR, Kong KH, Kim H, Kwon SH, Jeon JS, Han DC and Noh H: Sirt1-hypoxia-inducible factor-1α interaction is a key mediator of tubulointerstitial damage in the aged kidney. Aging Cell 18: e12904, 2019.
44. Abraham CR, Chen C, Cuny GD, Glicksman MA and Zeldich E: Small-molecule Klotho enhancers as novel treatment of neurodegeneration. Future Med Chem 4: 1671-1679, 2012.